

Supporting Information

Supporting Movie S1

This movie showed the rotation of four black brushes of the graphite oxide liquid crystal sample under the crossed polarizers to distinguish the sign of disclination. As presented in the movie, the negative disclination was determined because the brushes in the textures rotated in the opposite direction at the same angular velocity as the polarizers.

Supporting Movie S2

This movie showed the electric field-induced Freedericksz transition of graphite oxide liquid crystal under an external electric field (50 V). Once an electric field was applied, the transition could be clearly observed due to the sharp change of the color.

Materials and Methods

Materials

Graphite powder was obtained from Tianjin Guangfu Co. Ltd. The reagents including KMnO_4 , 98% sulfuric acid, phosphoric acid, 30% hydrogen peroxide aqueous solution and 36% hydrochloric acid were analytical grade and used as received.

Preparation of graphite oxide dispersion

Graphite oxide was prepared using an improved oxidization method with a small modification.¹ In brief, a mixture of graphite powder (3.0 g) and KMnO_4 (18.0 g) was slowly added into a 9:1 mixture of concentrated $\text{H}_2\text{SO}_4/\text{H}_3\text{PO}_4$ (360:40 mL). The suspension was heated to 50 °C, stirred for 12 h, cooled to room temperature and then poured into 400 mL ice water under stirring. Upon treatment with 8 mL 30 % H_2O_2 , the suspension turned into bright yellow. Successively, the suspension was sifted through a metal China Standard testing sieve (100 meshes, 150 μm) and then added with 200 mL of 30 % HCl solution. Repeated centrifugation and washing with a large amount of deionized water were conducted until the pH of the suspension was approximately neutral. We obtained a yellowish-brown aqueous dispersion of graphite oxide liquid crystals. The concentration of dispersion was measured from the amount of graphite oxide left after vacuum freeze drying.

Characterization of graphite oxide liquid crystal

Raman spectra were carried out using a Renishaw InVia Reflex spectrometer (Wotton-under-Edge, UK) with a 532 nm laser excitation. Atomic force microscopy (AFM) images of graphite oxide were taken in the tapping mode on a Nanoscope IV, with sample prepared by dispensing the extremely diluted dispersion into the freshly exfoliated mica substrates. Wide-angle X-ray diffraction (XRD) and small-angle X-ray diffraction (SAXS) analyses were performed on an X-ray diffractometer (D/MAX-2500, Rigaku Denki Co. Ltd., Japan). The XRD patterns with Cu $K\alpha$ radiation ($\lambda = 0.154056$ nm) at 40 kV and 100 mA were recorded in the range of $2\theta = 5-50^\circ$ for wide-angle XRD and $0.3-2^\circ$ for SAXS. Polarized optical microscopy (POM) images of graphite oxide liquid crystals were taken by observing the sample sealed between a pair of slide glasses under a pair of crossed polarizers. In order to maintain liquid crystalline structure, the samples for scanning electron microscopy (SEM) were obtained by dropping onto the glass slide, followed by freezing in liquid nitrogen and freeze-drying under vacuum. SEM images were captured at random locations of the sample. Microstructure and morphology of graphite oxide flakes were identified by a JEM-2100 transmission electron microscope (TEM, Tokyo, Japan) operated at 200 kV.

Tables and Figures

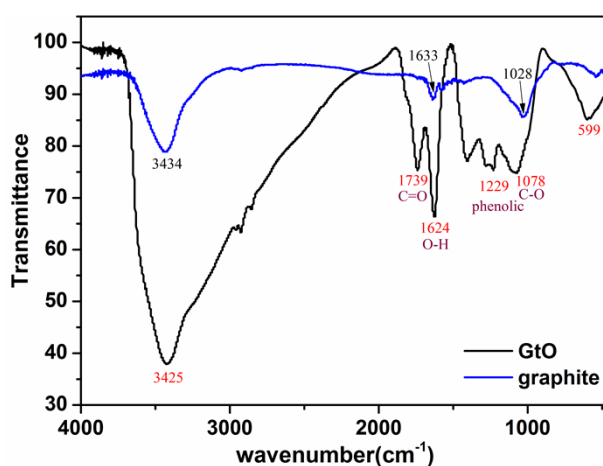


Figure S1. FTIR spectra of graphite and graphite oxide.

Table S1. Raman spectrum analysis of as-prepared graphite oxide.

	D position (cm ⁻¹)	G position (cm ⁻¹)	2D position (cm ⁻¹)	I_D/I_G	I_{2D}/I_G
Graphite oxide	1354	1591	2709	0.86	0.17

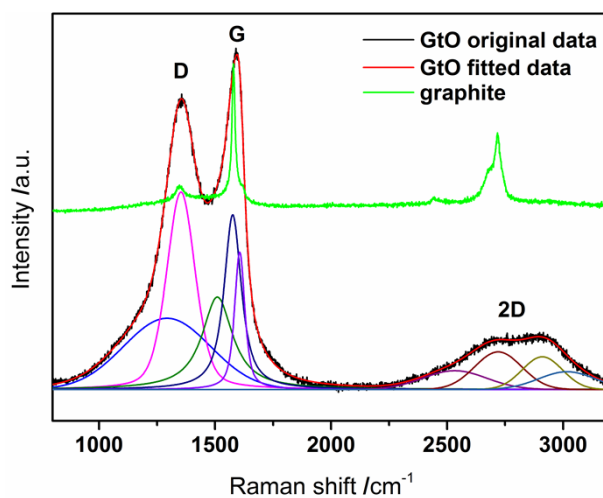


Figure S2. Raman spectra performed using an excitation laser wavelength of 532 nm. The black curve indicated the measured intensities and the red line represented the fitted Raman curve with the corresponding Raman bands.^{2,3} A combination of five bands (G, D₁, D₂, D₃, D₄) at about 1580, 1350, 1620, 1500 and 1200 cm⁻¹, respectively, was best suited for the first-order Raman spectra (1100-1700 cm⁻¹). The second-order spectra (2400-3300 cm⁻¹) were best fitted with bands at about 2450, 2700, 2900 and 3000 cm⁻¹.

Raman spectrum of as-prepared GtO shown in Fig. S2 displayed the D and G band at 1354 and 1591 cm⁻¹, respectively. In comparison with previous report,⁴ the smaller I_D/I_G peak intensity ratio (0.86) was obtained, which indicated the lower defects and disorders of our prepared GtO structure.

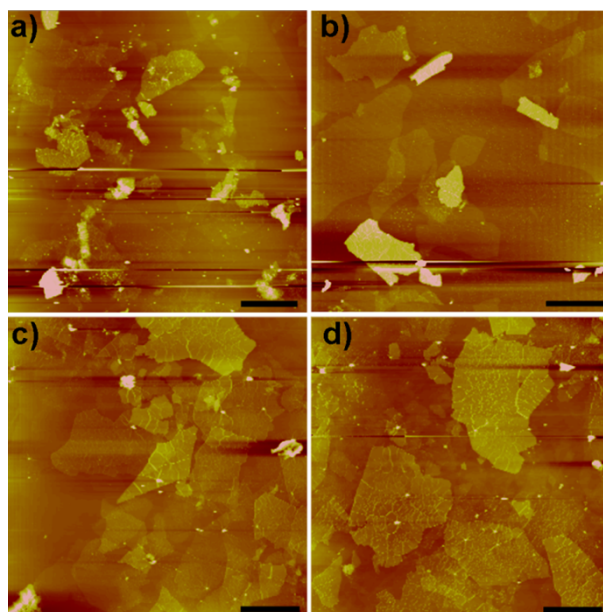


Figure S3. Representative AFM images of graphite oxide flakes (a-d) deposited on the fresh exfoliated mica from the aqueous dispersions. From AFM images, 311 pieces of graphite oxide flakes were used to statistically calculate their lateral width (W) and the thickness (T). The number-average width $\langle W \rangle$ and $\langle T \rangle$ were determined on the basis of these statistical data. The relative standard deviation (σ_w) was calculated by the formula $\sigma_w = (\langle W^2 \rangle - \langle W \rangle^2)^{1/2} / \langle W \rangle$, where the notation of ' $\langle \rangle$ ' represented the number average function. The relative standard deviation (σ_T) was evaluated in the same way. Scale bar depicted 10 μm .

Table S2. Characteristics sizes of GtO flakes as determined from AFM.

	$\langle W \rangle / \mu\text{m}$	σ_w	$\langle T \rangle / \text{nm}$	σ_T	Aspect ratio
GtO	7.20 ± 4.79	0.67	11.84 ± 10.43	0.88	ca. 600

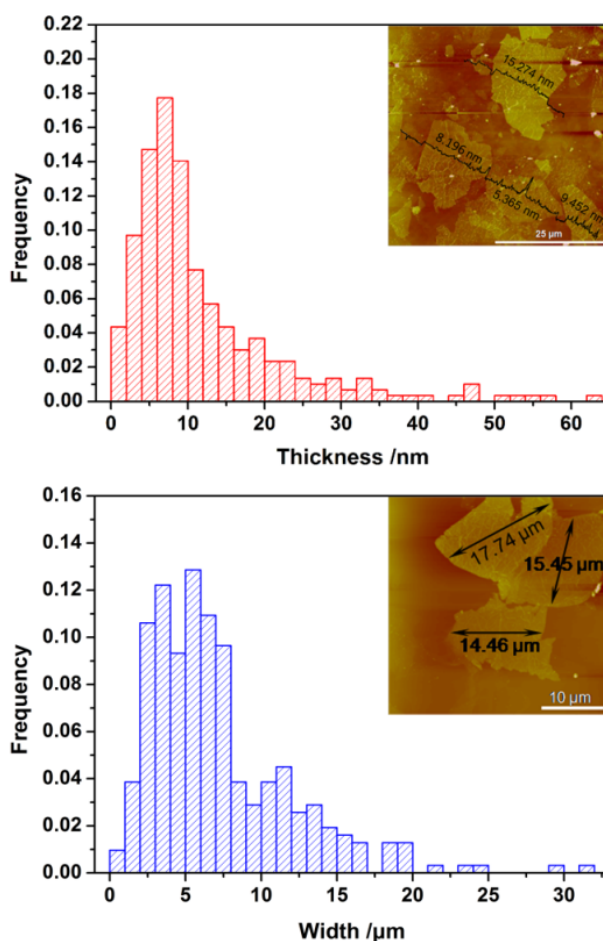


Figure S4. Top: The thickness distribution of GtO flakes was estimated statistically from AFM images including 311 pieces of GtO flakes, as presented in Figure S3. Bottom: The width distribution of GtO flakes was calculated by the above mentioned method. The insets depicted the representative AFM thickness image and width image of GtO flakes, respectively.

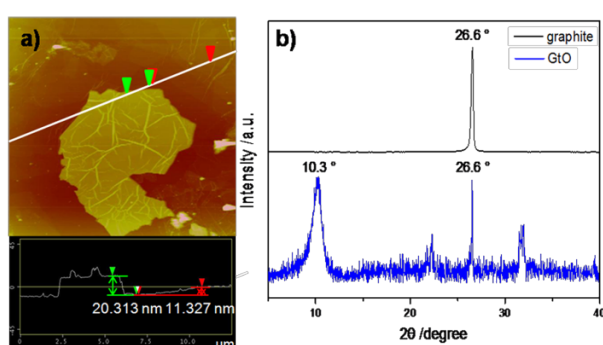


Figure S5. a) Representative AFM image of graphite oxide aqueous dispersions showed the thickness of graphite oxide flakes. The section line analysis gave the thicknesses of graphite oxide flakes as 20.313 nm and 11.327 nm, respectively, indicating that a graphite oxide flake was composed of about a dozen layers. b) XRD spectra of graphite and graphite oxide. The average thickness of graphite oxide flakes was calculated by the Scherrer formula: $T(hkl) \text{ (nm)} = K\lambda / (\beta \cos(\theta_{hkl}))$, where $\lambda(\text{CuK}\alpha) = 0.154 \text{ nm}$; $\beta =$ peak width at half height (rad); $\theta_{hkl} =$ Bragg angle ($^\circ$); $K = 0.9$, instrumental factor. The peak at $26.6^\circ 2\theta$ of the GtO XRD pattern indicated that the sample might include some unoxidized graphite, which should be removed because the presence of graphite would influence on the alignment of GtO LCs.

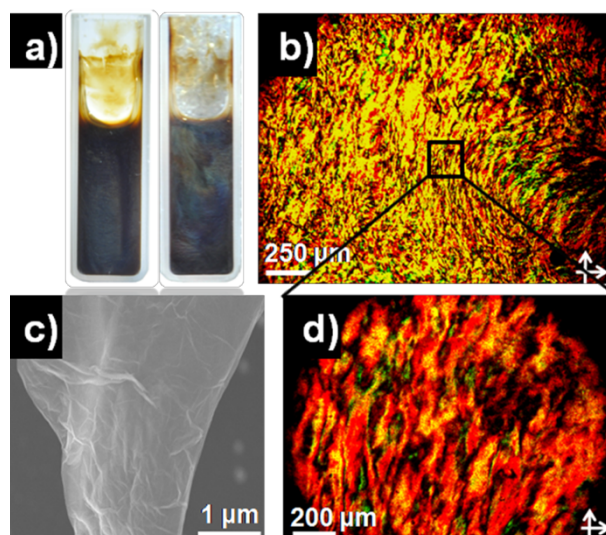


Figure S6. a) Typical micrograph of 1.45 wt% graphite oxide aqueous dispersion. Left: a lamellar feature (the sample was kept stationary for more than a week). Right: a colorful feature after agitation. b) Typically nematic texture of graphite oxide liquid crystals under crossed polarizers. A wavelike pattern was clearly seen in this image. The marked area (rectangle in b) was zoomed in as d). Transmitted polarized light with analyser and polarizer crossed at 0° in b) and d). c) SEM image of wrinkled graphite oxide flakes showed that a graphite oxide flake was composed of several sheets.

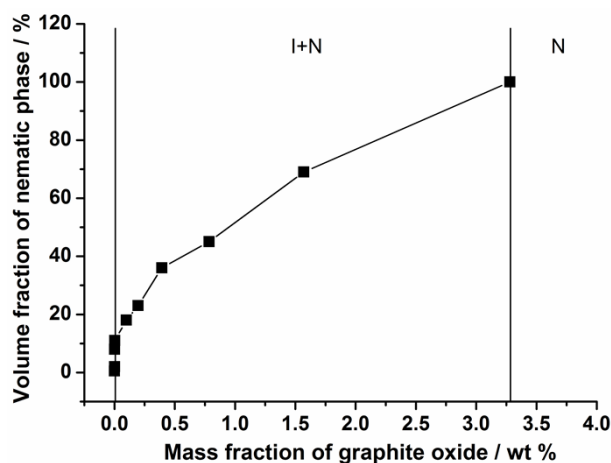


Figure S7. Phase diagram of GtO aqueous dispersions with an aspect ratio of roughly 600.

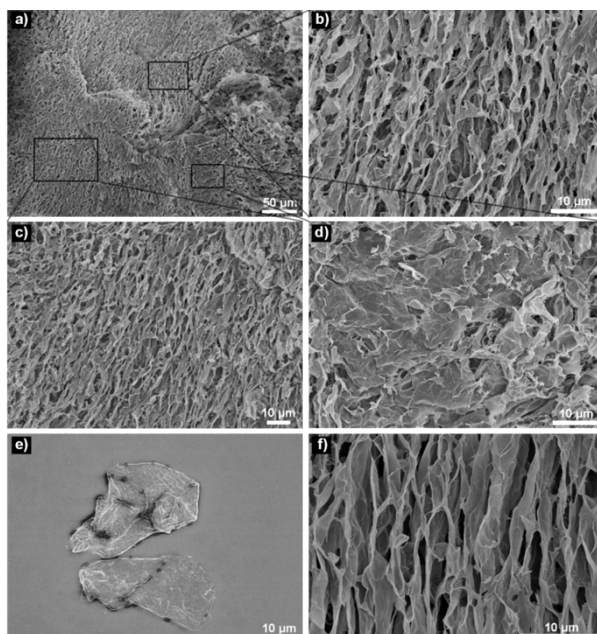


Figure S8. SEM images of graphite oxide aqueous dispersions. a) SEM image of graphite oxide liquid crystal. The marked areas were zoomed in as b), c) and d), respectively, indicating the different alignment directions. b) and c) were perpendicular to the surface, while d) was planar to the surface. e) Micrograph of large graphite oxide flakes. f) Lamellar texture of graphite oxide liquid crystals (~ 1.45 wt %).

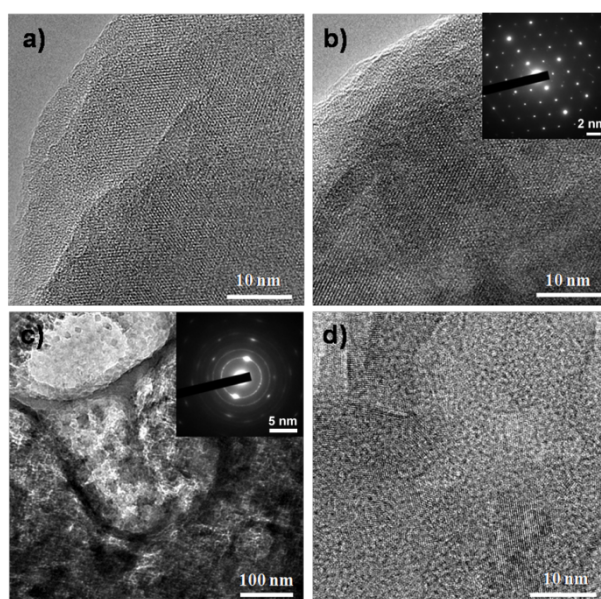


Figure S9. TEM images of GtO LCs dropped onto copper grids and the corresponding selected area electron diffraction (SAED) patterns (insets). a) TEM image of a GtO flake taken at the relatively flat edge of the sample. b) TEM image of GtO flakes with a high degree of ordering and the corresponding SAED pattern (spot pattern). c) TEM image of GtO flakes over a large domain and the corresponding SAED pattern (ring pattern). d) TEM image of randomly oriented GtO flakes showing the anisotropy of GtO LCs.

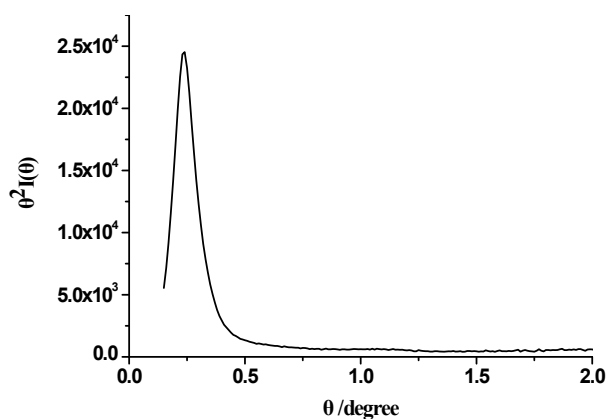


Figure S10. The SAXS profile of GtO LCs sample.

SAXS analysis has become an important approach to the study of highly ordered nanostructured materials. Here, SAXS data was acquired for GtO LCs to further investigate the alignment of GtO flakes. Obviously, there was a single sharp peak at $\theta=0.236^\circ$ in the SAXS profile, illustrating that the GtO LCs exhibited a long-period ordered structure, which agreed well with the POM and SEM images.

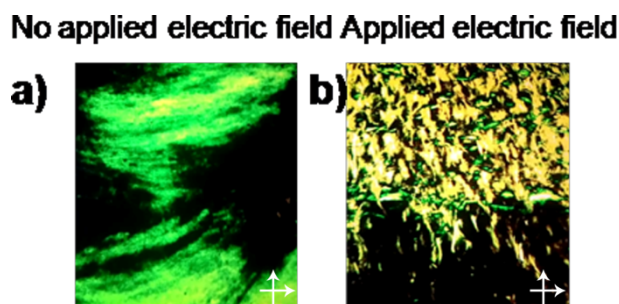


Figure S11. Liquid crystal texture of GtO without a) and with b) applied electric field of 50 V.

References

- 1 D. C. Marcano, D. V. Kosynkin, J. M. Berlin, A. Sinitskii, Z. Sun, A. Slesarev, L. B. Alemany, W. Lu and J. M. Tour, *ACS Nano*, 2010, **4**, 4806.
- 2 G. A. Zickler, B. Smarsly, N. Gierlinger, H. Peterlik and O. Paris, *Carbon*, 2006, **44**, 3239-3246.
- 3 A. Sadezky, H. Muckenhuber, H. Grothe, R. Niessner and U. Pöschl, *Carbon*, 2005, **43**, 1731-1742.
- 4 W. Gao, L. B. Alemany, L. Ci and P. M. Ajayan, *Nature chemistry*, 2009, **1**, 403-408.